Trans. Tianjin Univ. 2011, 17: 006-012
DOI 10.1007/s12209-011-1469-8

Active Control of Free Paraboloidal Membrane Shells Using Photostrictive Actuators*

WANG Xinjie(王新杰)[1,2], YUE Honghao(岳洪浩)[1,2], DENG Zongquan(邓宗全)[1,2]
(1. State Key Laboratory of Robotics and Systems, Harbin Institute of Technology, Harbin 150080, China;
2. Research Center of Aerospace Mechanism and Control, Harbin Institute of Technology, Harbin 150001, China)

Abstract: The paraboloidal membrane shell with free boundary condition is actively controlled using photostrictive actuators which can provide contactless actuation under the illumination of ultraviolet light. The governing equations of the paraboloidal shell laminated with paired photostrictive actuators are established based on membrane approximation. The modal control actions of meridional/circumferential actuators are respectively formulated and evaluated by case studies. Constant light intensity related to the velocity of the shell is adopted, and then the governing equations are written in a closed-loop form which can be solved with Newmark-β method. Considering the multi-field coupling behavior of photostrictive actuators, time histories of transverse displacement and control light intensity are simulated and evaluated. The results show that photostrictive actuators can effectively control the vibration of the paraboloidal membrane shell, and the photostrictive actuators oriented along circumferential direction can give better control effect than photostrictive actuators placed along the meridional direction.

Keywords: photostrictive actuator; paraboloidal shell; active control; membrane approximation

Paraboloidal shells with good dynamical behaviors and focusing characteristics are commonly utilized in the fields of mechanical, architectural and aeronautical engineering. Sometimes, paraboloidal shells are fabricated as flexible and low damping components which need to be micro-controlled. Based on the vibration characteristics of paraboloidal shells and development of smart materials, the paraboloidal shells laminated with smart materials have been studied. Distributed sensation and actuation of paraboloidal shells with simply supported boundary and free boundary condition were investigated by Tzou and Ding[1,2]. The free-floating paraboloidal membrane shells laminated with piezoelectric actuator patches were studied by Yue, Deng and Tzou[3-5]. In these references, the piezoelectric actuator patches were used as sensors and actuators, but the piezoelectric actuator patches have some deficiencies, such as electrical noise and additional weight induced by lead wires[6]. The photostrictive materials with the wireless non-contact nature can exhibit advantages under these situations.

Among photostrictive materials, PLZT ceramic has been researched widely because of its easy fabrication and relatively high photostriction[7]. Through converting the light directly into mechanical motion, the PLZT ceramic can be applied to non-contact micro-actuation. A micro walking device and photo-driven relay were demonstrated by Uchino[8]. A prototype of optical microgripper was developed by Fukuda *et al*[9]. To improve the response speed and precision of the optical actuator system, double side irradiation scheme and prediction of on-off control were implemented and confirmed by Fukuda and Morikawa[10,11]. Poosanaas introduced a solar tracking device for future space missions[12]. And the PLZT bimorph was also used in an optical servo system by Liang *et al*[13]. Furthermore, photostrictive materials used in structronic systems have been found in a series of references[14-18]. Shih and Tzou also investigated the effects of photostrictive actuator locations on simply supported paraboloidal shell with approximate equivalent spherical shell model[19]. However, the photostrictive laminated paraboloidal membrane shells with free boundary condition need to be further investigated.

This paper presents an investigation into the precision actuation and vibration control of paraboloidal membrane shells using photostrictive actuators. Based on membrane approximation, modal governing equations of

Accepted date: 2010-04-14.
*Supported by National Natural Science Foundation of China (No. 50705017) and the "111 Project" (No. B07018).
WANG Xinjie, born in 1982, male, doctorate student.
Correspondence to WANG Xinjie, E-mail: wxj_hit@163.com.

the paraboloidal shells laminated with photostrictive actuators are formulated first. The modal control actions of meridional/circumferential actuators are evaluated by case studies. To induce both positive and negative control force, paired photostrictive actuators placed on the top and bottom surfaces of paraboloidal shells respectively are actuated by constant intensity light. The governing equation is solved with Newmark-β method considering the behavior of photostrictive actuators. Time history responses of transverse displacement and control light intensity are also presented and analyzed in this paper.

1 Modeling of paraboloidal membrane shell laminated with photostrictive actuators

The mathematical model of a paraboloidal shell laminated with photostrictive actuators is presented in this section. A tri-orthogonal coordinate system (ϕ, ψ, α_3) is employed, where ϕ, ψ, α_3 denote the meridional, circumferential and transverse directions. As shown in Fig.1, if a and c represent the radial distance and meridian height at the pole respectively, constant b can be represented as $b = 2a/c$. The two principal radii of the double curvature are $R_\phi = b/\cos^3\phi$ and $R_\psi = b/\cos\phi$. Lamé parameters of the shell are $A_1 = b/\cos^3\phi$ and $A_2 = (b\sin\phi)/\cos\phi$.

For paraboloidal membrane shells, membrane approximation is applied, i.e., all the bending components are neglected. If there is no excitation force, system equations of the paraboloidal membrane shell can be written as[3]

$$\frac{\partial(N^m_{\phi\phi}\tan\phi)}{\partial\phi}+\frac{1}{\cos^3\phi}\frac{\partial N^m_{\psi\phi}}{\partial\psi}-\frac{N^m_{\psi\psi}}{\cos^2\phi}=\frac{b\sin\phi}{\cos^4\phi}\rho h\frac{\partial^2 u_\phi}{\partial t^2} \quad (1)$$

$$\frac{\partial(N^m_{\phi\psi}\tan\phi)}{\partial\phi}+\frac{1}{\cos^3\phi}\frac{\partial N^m_{\psi\psi}}{\partial\psi}+\frac{N^m_{\psi\phi}}{\cos^2\phi}=\frac{b\sin\phi}{\cos^4\phi}\rho h\frac{\partial^2 u_\psi}{\partial t^2} \quad (2)$$

$$-N^m_{\phi\phi}\tan\phi-\frac{N^m_{\psi\psi}\tan\phi}{\cos^2\phi}=\frac{b\sin\phi}{\cos^4\phi}\rho h\frac{\partial^2 u_3}{\partial t^2} \quad (3)$$

where N^m_{ij} is mechanical force; ρ mass density of the paraboloidal shell; h thickness of the shell; u_ϕ, u_ψ and u_3 are the corresponding displacement along ϕ, ψ and α_3 direction. The oscillation of paraboloidal shells may be different under different boundary conditions. In this paper, the paraboloidal shell to be studied is completely free. Since the transverse oscillation of the paraboloidal shell dominates in the dynamical analysis, only transverse vibration is actively controlled by photostrictive actuators in this paper. According to Ref.[4], mode shape function U_{3k} of the paraboloidal membrane shell in the transverse direction is constructed as

$$U_{3k} = A_k(k+1)\cos\phi\sin^k\phi\cos(k\psi) \quad (4)$$

where k is the mode number and A_k is the kth modal amplitude.

To induce both positive and negative control force, paired photostrictive actuators are placed on the top and bottom surfaces of the paraboloidal shell respectively as shown in Fig.2. The actuators are defined by the coordinates (ϕ_1^*, ψ_1^*) and (ϕ_2^*, ψ_2^*). Because the paraboloidal shell is studied herein based on membrane approximation, the control moments induced by the photostrictive actuators are neglected. The photostrictive actuators used in this paper are uni-axial, and they can only give control effect along the polarity direction. If the actuator systems are supposed to provide control force $N^a_{\phi\phi}$, the actuators

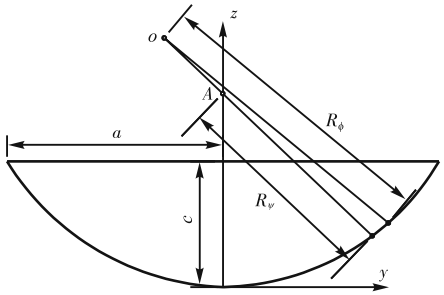

Fig.1 Cross-section of paraboloidal shell

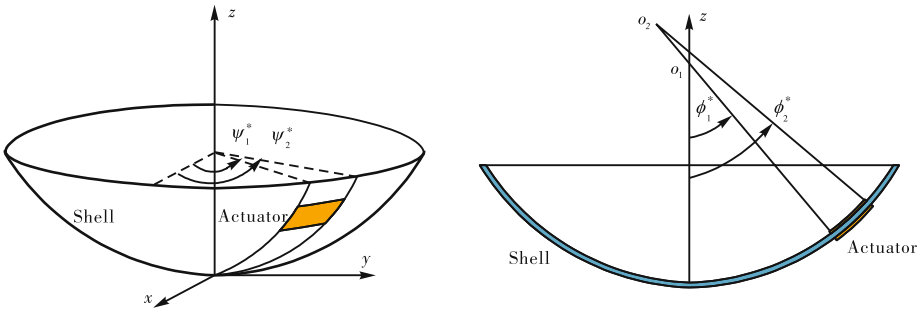

Fig.2 Paraboloidal shell laminated with photostrictive actuators

should be placed in ϕ direction (ϕ-actuator). If the photostrictive laminated structronic system needs control force $N^a_{\psi\psi}$, the photostrictive actuators should be oriented in ψ direction (ψ-actuator).

For the paraboloidal shell, the control moment of photostrictive actuators can be neglected because of the small bending effect[19]. So the transverse governing equation of the photostrictive laminated paraboloidal membrane shell can be given as

$$\frac{\cos^3\phi}{b}N^m_{\phi\phi}+\frac{\cos\phi}{b}\quad N^m_{\psi\psi}+\rho h\frac{\partial^2 u_3}{\partial t^2}=\frac{\cos^3\phi}{b}N^a_{\phi\phi}$$

(ϕ-actuator) (5a)

$$\frac{\cos^3\phi}{b}N^m_{\phi\phi}+\frac{\cos\phi}{b}N^m_{\psi\psi}+\rho h\frac{\partial^2 u_3}{\partial t^2}=\frac{\cos\phi}{b}N^a_{\psi\psi}$$

(ψ-actuator) (5b)

The control force $N^a_{\phi\phi}$ and $N^a_{\psi\psi}$, induced by photostrictive actuators in Fig.2, can be represented as[18]

$$N^a_{\phi\phi}=h_a Y_a\bar{S}[u_s(\phi-\phi^*_1)-u_s(\phi-\phi^*_2)]\cdot$$
$$[u_s(\psi-\psi^*_1)-u_s(\psi-\psi^*_2)]$$

(ϕ-actuator) (6a)

$$N^a_{\psi\psi}=h_a Y_a\bar{S}[u_s(\phi-\phi^*_1)-u_s(\phi-\phi^*_2)]\cdot$$
$$[u_s(\psi-\psi^*_1)-u_s(\psi-\psi^*_2)]$$

(ψ-actuator) (6b)

where u_s is a unit step function; $\bar{S}$ the strain of the photostrictive actuators; Y_a the Young's modulus of photostrictive actuator; h_a the thickness of the actuator. Assume that the transverse response is composed of all participating modes, i.e., $u_3(\phi,\psi,t)=\sum_{k=1}^{\infty}\eta_k(t)U_{3k}$, where η_k is the kth modal participation factor. Using modal expansion method[20], the kth modal equation of the paraboloidal shell in the transverse direction can be obtained as

$$\ddot{\eta}_k+2\xi_k\omega_k\dot{\eta}_k+\omega_k^2\eta_k=F_k^c \tag{7}$$

where ξ_k is the kth modal damping ratio; ω_k the kth modal natural frequency of the paraboloidal shell; F_k^c the kth modal control force. According to Eq.(5), the control force can be presented as

$$F_k^c=\frac{1}{\rho h N_k}\iint_{\psi\ \phi}\frac{\cos^3\phi}{b}N^a_{\phi\phi}U_{3k}\frac{b^2\sin\phi}{\cos^4\phi}\mathrm{d}\phi\mathrm{d}\psi=$$
$$\frac{A_k(k+1)h^aY_a\bar{S}b}{\rho h N_k}\frac{[\sin(k\psi_2^*)-\sin(k\psi_1^*)]}{k}\cdot$$
$$\int_{\phi_1^*}^{\phi_2^*}\sin^{(k+1)}\phi\,\mathrm{d}\phi=(F_k^c)_\phi\bar{S}\quad(\phi\text{-actuator}) \tag{8a}$$

$$F_k^c=\frac{1}{\rho h N_k}\iint_{\psi\ \phi}\frac{\cos\phi}{b}N^a_{\psi\psi}U_{3k}\frac{b^2\sin\phi}{\cos^4\phi}\mathrm{d}\phi\mathrm{d}\psi=$$
$$\frac{A_k(k+1)h^aY_a\bar{S}b}{\rho h N_k}\frac{[\sin(k\psi_2^*)-\sin(k\psi_1^*)]}{k}\cdot$$
$$\int_{\phi_1^*}^{\phi_2^*}\frac{\sin^{(k+1)}\phi}{\cos^2\phi}\mathrm{d}\phi=(F_k^c)_\psi\bar{S}\quad(\psi\text{-actuator}) \tag{8b}$$

where $(F_k^c)_\phi$ and $(F_k^c)_\psi$ represent the modal control action in ϕ and ψ direction respectively. N_k is determined as

$$N_k=\iint_{\psi\ \phi}U_{3k}^2\frac{b^2\sin\phi}{\cos^4\phi}\mathrm{d}\phi\mathrm{d}\psi=$$
$$A_k^2b^2(k+1)^2\pi\int_0^{\phi^*}\frac{\sin^{(2k+1)}\phi}{\cos^2\phi}\mathrm{d}\phi \tag{9}$$

where ϕ^* is meridional angle of boundary rim.

2 Active control of photostrictive laminated paraboloidal shell

The photostrictive actuators can be activated under high energy light illumination. If control light intensity, which is decided according to some control laws, is used as control input, the paraboloidal shell can be actively controlled by the photostrictive actuators. In this paper, light intensity is related to modal velocity, and then the governing equation can be written in a closed-loop form. In this way, Eq.(7) can be written in another form:

$$\ddot{\eta}_{kj}+2\xi_k\omega_k\dot{\eta}_{kj}+\omega_k^2\eta_{kj}=F_{kj}^c \tag{10}$$

where subscript j denotes the time instant t_j. Eq.(10) can be solved with Newmark-β method[21].

$$K_{eq}=a_0+2a_1\xi_k\omega_k+\omega_k^2 \tag{11a}$$

$$F_{eq\,j}=F_{kj}^c+(a_0\eta_{k(j-1)}+a_2\dot{\eta}_{k(j-1)}+a_3\ddot{\eta}_{k(j-1)})+$$
$$2\xi_k\omega_k(a_1\eta_{k(j-1)}+a_4\dot{\eta}_{k(j-1)}+a_5\ddot{\eta}_{k(j-1)}) \tag{11b}$$

$$\eta_{kj}=F_{eq\,j}/K_{eq} \tag{11c}$$

$$\ddot{\eta}_{kj}=a_0(\eta_{kj}-\eta_{k(j-1)})-a_2\dot{\eta}_{k(j-1)}-a_3\ddot{\eta}_{k(j-1)} \tag{11d}$$

$$\dot{\eta}_{kj}=\dot{\eta}_{k(j-1)}+a_6\ddot{\eta}_{k(j-1)}+a_7\ddot{\eta}_{kj} \tag{11e}$$

$$a_0=\frac{1}{b_1\Delta t^2},\quad a_1=\frac{b_2}{b_1\Delta t},\quad a_2=\frac{1}{b_1\Delta t},$$
$$a_3=\frac{1}{2b_1}-1,\quad a_4=\frac{b_2}{b_1}-1,\quad a_5=(\frac{b_2}{2b_1}-1)\Delta t,$$
$$a_6=(1-b_2)\Delta t,\quad a_7=b_2\Delta t \tag{11f}$$

where K_{eq} and F_{eq} are equivalent stiffness and equivalent control force respectively; Δt is time step; b_1 and b_2 are

constants of Newmark-β method. Control force F_{kj}^{c} at t_j can be written as

$$F_{kj}^{c} = -\mathrm{sgn}(\dot{\eta}_{k(j-1)})\left|(F_k^{c})_{\phi}\right|\bar{S}(t_j) \quad (\phi\text{-actuator}) \tag{12a}$$

$$F_{kj}^{c} = -\mathrm{sgn}(\dot{\eta}_{k(j-1)})\left|(F_k^{c})_{\psi}\right|\bar{S}(t_j) \quad (\psi\text{-actuator}) \tag{12b}$$

where sgn $(\cdot)$ is a signum function, $\mathrm{sgn}(x)=1$ when $x>0$; $\mathrm{sgn}(x)=0$ when $x=0$; $\mathrm{sgn}(x)=-1$ when $x<0$.

Strain $\bar{S}(t_j)$ induced by photostrictive actuator can be defined as[16]

$$\bar{S}(t_j) = d_{33}\left[E_1(t_j) + \frac{P_n}{\varepsilon}\theta(t_j)\right] - \lambda\theta(t_j)/Y_a \tag{13a}$$

$$E_1(t_j) = E_1(t_{j-1}) + \{[E_s - E_1(t_{j-1})]\frac{\alpha}{a_s}\cdot I(t_j)\mathrm{e}^{-\frac{\alpha}{a_s}I(t_j)\Delta t} - E_1(t_{j-1})\beta\mathrm{e}^{-\beta\Delta t}\}\Delta t \tag{13b}$$

$$\theta(t_j) = \theta(t_{j-1}) + \{[I(t_j)P - \gamma\theta(t_{j-1})]\Delta t\}/\ (H+\Delta t) \tag{13c}$$

where $E_1(t_j)$ is photo-induced electric field; $\theta(t_j)$ temperature heated by high energy light; P_n pyroelectric constant; ε electric permittivity; d_{33} piezoelectric strain constant; λ stress-temperature constant; E_s is saturated electric field; a_s aspect ratio of single patch actuator (length/width); α optical actuator constant; $I(t_j)$ light intensity at time t_j; β voltage leakage constant; P power of absorbed heat; γ heat transfer rate; and H heat capacity of optical actuator.

In this paper, constant light intensity control is used. The amplitude of light intensity is constant and can be determined as

$$I(t_j) = G_1[\max|\dot{\eta}_k(t)|] \tag{14}$$

where G_1 is light intensity gain. As mentioned above, paired actuators are laminated with the paraboloidal shell. So light direction should be alternatively applied to the top and bottom photostrictive actuators depending on velocity direction. When the paraboloidal shell oscillates downward, light should be applied to the bottom actuators, then positive control force can be induced; when the paraboloidal shell oscillates upward, light should be applied to the top actuators, and negative control force can be induced. It is assumed that the remanent strain and electric field of actuators can disappear immediately when light direction is changed.

3 Case studies

In this section, the modal control actions are analyzed and evaluated firstly while the actuator's location varies along the meridional and circumferential direction. The time history responses are presented based on the control laws introduced in the previous section. A shallow paraboloidal shell is taken as a sample model. The paraboloidal shell is made of Plexiglas (Y=3.1×10^9 N/m^2, ρ = 1 190 kg/m^3 and μ = 0.35) and the geometric parameters are a = 0.2 m, c = 0.1 m, h = 1×10^{-3}m. All the photostrictive actuators are uniformly thin with the thickness h_a = 1×10^{-4} m. And the material properties of photostrictive actuators are listed in Tab.1[16].

Tab.1 Material properties of photostrictive actuators

Parameter	Value
Saturated electric field E_s/(V·m^{-1})	2.43×10^5
Young's modulus Y_a/(N·m^{-2})	6.3×10^{10}
Optical actuator constant α/(m^2·W^{-1}·s^{-1})	2.772×10^{-3}
Voltage leakage constant β/(V·s^{-1})	0.01
Power of absorbed heat P/(m^2·s^{-1})	0.023
Piezoelectric strain constant d_{33}/(m·V^{-1})	1.79×10^{-10}
Heat capacity H/(W·℃$^{-1}$)	16
Heat transfer rate γ/(W·℃$^{-1}$·s^{-1})	0.915
Stress-temperature constant λ/(N·m^{-2}·℃$^{-1}$)	6.808 6×10^4
Pyroelectric constant P_n/(C·m^{-2}·℃$^{-1}$)	0.25×10^{-4}
Electric permittivity ε/(F·m^{-1})	1.65×10^{-8}

3.1 Modal control action analysis

The location of photostrictive actuator varies from 0 to ϕ^* with step 0.1. And the location of the actuator in circumferential direction varies from 0 to 2π with step 0.1. The photostrictive actuator patches can be defined with $\Delta\phi = \phi_2^* - \phi_1^* = 0.1$ and $\Delta\psi = \psi_2^* - \psi_1^* = 0.1$. For convenience, modal amplitude A_k is supposed to be 1. The modal control actions of ϕ-actuator and ψ-actuator are presented in Fig.3—Fig.6, which show that the modal control action of ψ-actuator is larger than that of ϕ-actuator. Along meridional direction, much larger modal control action can be induced by the photostrictive actuators when the locations of actuators are close to the rim of the shell. Along circumferential direction, the locations with large or tiny modal control action can be determined according to Fig.3—Fig.6. The placement of actuators is one of the critical problems in structural active control. Based on Fig.3—Fig6, one can select the location where the photostrictive actuators can provide good control effect.

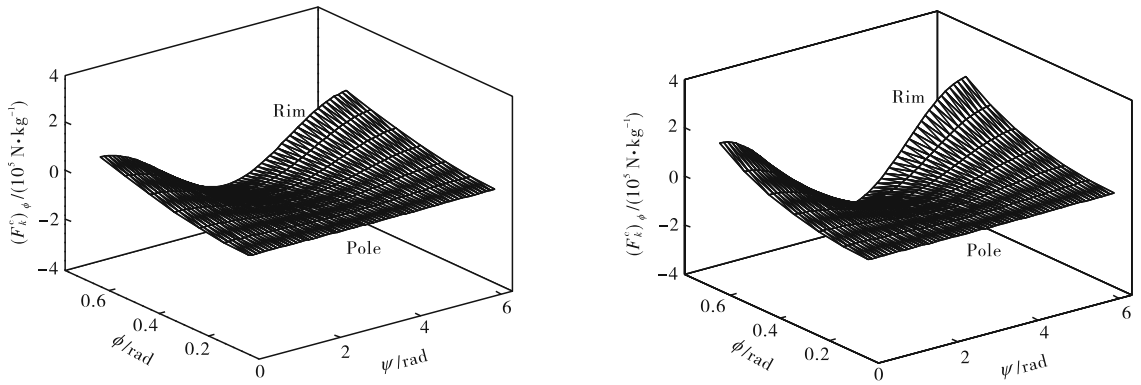

(a) Modal control action of ϕ -actuator (b) Modal control action of ψ-actuator

Fig.3 Modal control action for free paraboloidal membrane shell when k=1

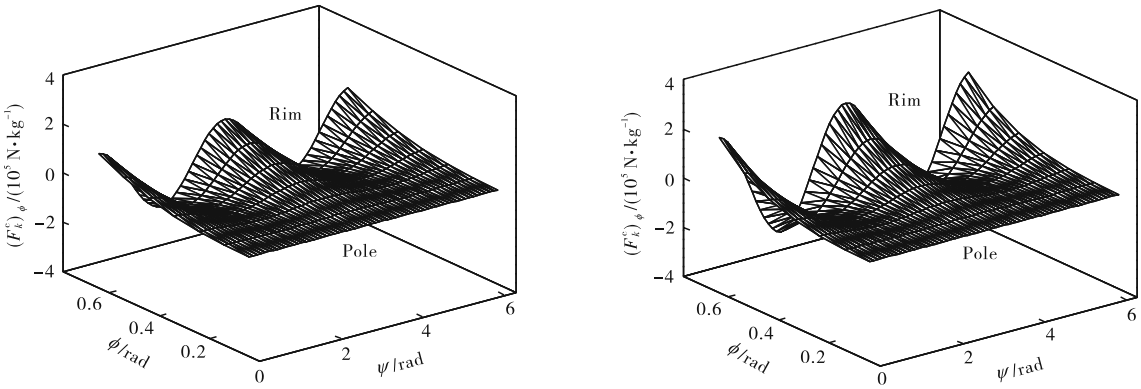

(a) Modal control action of ϕ -actuator (b) Modal control action of ψ-actuator

Fig.4 Modal control action for free paraboloidal membrane shell when k=2

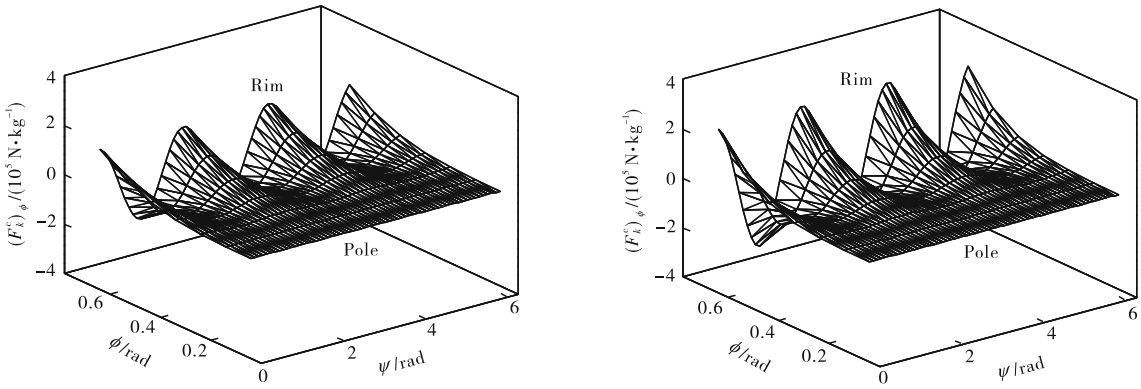

(a) Modal control action of ϕ -actuator (b) Modal control action of ψ-actuator

Fig.5 Modal control action for free paraboloidal membrane shell when k=3

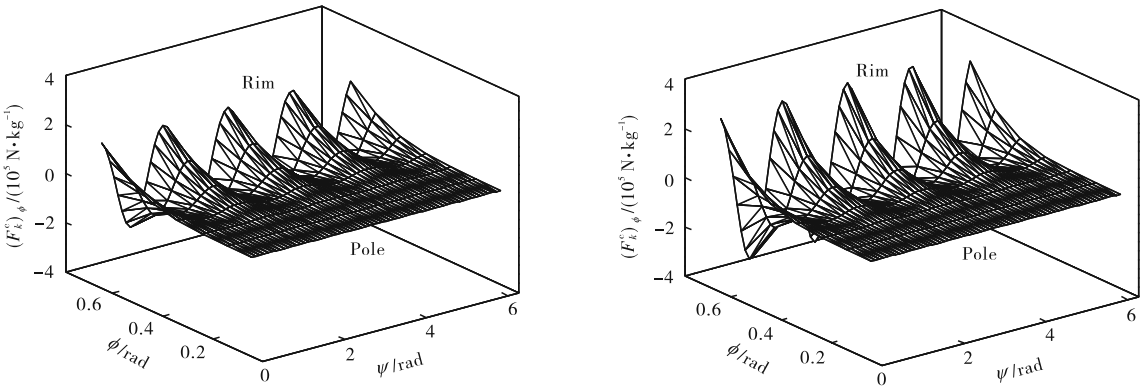

(a) Modal control action of ϕ -actuator (b) Modal control action of ψ-actuator

Fig.6 Modal control action for free paraboloidal membrane shell when k=4

3.2 Time history analysis

In this section, time histories of displacement and control light intensity are analyzed. As discussed above, the actuators at different locations provide different control forces. To induce large control force and provide good control effect, the location of paired photostrictive actuators is defined as $\phi_1^* = 0.70$, $\phi_2^* = 0.75$, $\psi_1^* = \pi - 0.1$, $\psi_2^* = \pi + 0.1$. Polarities of actuators are all in circumferential direction because of their better control effect. Two modes (k=3, 4) are studied as examples in this paper. The frequencies of these two modes can be calculated with ANSYS (k=3, f=22.70 Hz and k=4, f =41.07 Hz). The effect of actuator stiffness can be neglected here. One location of the shell ($\phi = 0.73, \psi = \pi$) is used as the reference point for control simulation. To observe the displacement response of the reference point, an initial displacement of 1.0×10^{-3} m and initial damping ratio of 1% are imposed. The 10% of the settling time of responses is set for comparing the control effect.

Fig.7 illustrates the displacement responses of the membrane shell with or without ϕ-actuators. For k=3 mode, the settling time corresponding to controlled response is 0.750 s, which reveals a great improvement when compared with free response (1.630 s). And the control damping ratio for k=3 mode is 0.017. For k=4 mode, the settling time corresponding to free and controlled response are 0.901 s and 0.610 s respectively. And the damping ratio for k=4 mode is 0.012. With the control scheme mentioned above, the control light applied to the top and bottom actuator is shown in Fig.8. The direction of control light should be adjusted carefully; otherwise, the vibration of the paraboloidal shell cannot be suppressed, even amplified.

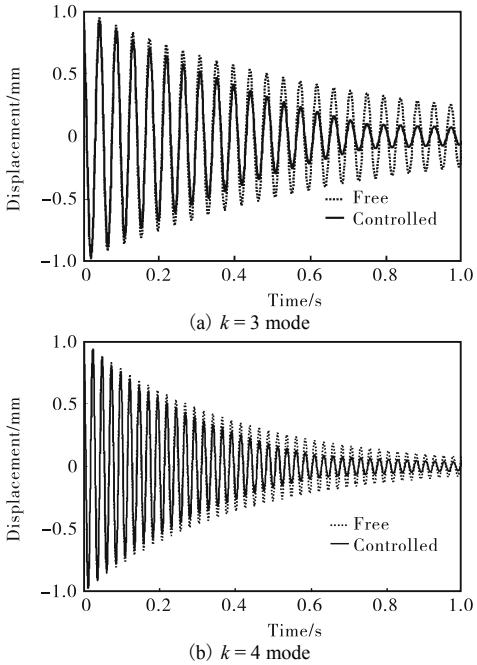

Fig.7 Time history of displacement responses

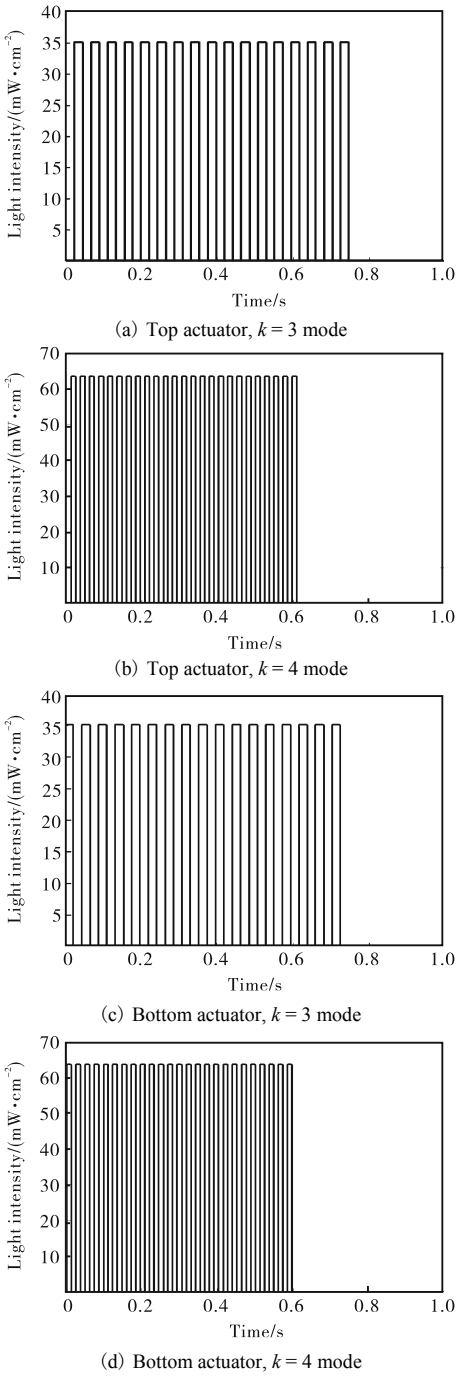

Fig.8 Time histories of light intensity applied to actuators

4 Conclusions

In this paper, the paraboloidal membrane shell is actively controlled by photostrictive actuators with the characteristic of non-contact actuation. Considering the nonlinearity of photostrictive actuators, governing equations of the structronic system are solved with Newmark-

β method. In case studies, the modal control action of ϕ-actuator is larger than that of ψ-actuator. So photostrictive actuators should be arranged with polarities along circumferential direction of the paraboloidal shell. Meanwhile, the proper location for photostrictive actuators to provide good control effect can be decided based on modal control actions as shown in Fig.3—Fig.6. Considering the actuator's behavior, numerical simulation with constant light intensity control is implemented. Time history analyses suggest that the transverse vibration of the paraboloidal shell with low frequency can be suppressed by photostrictive actuators. And the direction of control light is crucial for the vibration control of photostrictive laminated structure.

References

[1] Tzou H S, Ding J H. Actuator placement and micro-actuation efficiency of adaptive paraboloidal shells[J]. *Journal of Dynamic Systems*, *Measurement and Control*, 2003, 125(4): 577-584.

[2] Ding J H, Tzou H S. Micro-electromechanics of sensor patches on free paraboloidal shell structronic systems[J]. *Mechanical Systems and Signal Process*, 2004, 18(2): 367-380.

[3] Yue H H, Deng Z Q, Tzou H S. Distributed signal analysis of free-floating paraboloidal membrane shells[J]. *Journal of Sound and Vibration*, 2007, 304(3-5): 625-639.

[4] Yue H H, Deng Z Q, Tzou H S. Optimal actuator locations and precision micro-control actions on free paraboloidal membrane shells[J]. *Communications in Nonlinear Science and Numerical Simulation*, 2008, 13(10): 2298-2307.

[5] Yue H H, Deng Z Q, Tzou H S. Spatially distributed modal signals of free shallow membrane shell structronic system[J]. *Communications in Nonlinear Science and Numerical Simulation*, 2008, 13(9): 2041-2050.

[6] Tzou H S, Liu B J, Cseledy D. Optopiezothermoelastic actions and micro-control sensitivity analysis of cylindrical opto-mechanical shell actuators[J]. *Journal of Theoretical and Applied Mechanics*, 2002, 40 (3): 775-796.

[7] Sun D, Tong L. Modeling of wireless remote shape control for beams using nonlinear photostrictive actuators[J]. *International Journal of Solids and Structures*, 2007, 44(2): 672-684.

[8] Uchino K. Photostrictive actuator[C]. In: *Proceedings of IEEE Ultrasonics Symposium*. Honolulu, USA, 1990. 721-723.

[9] Fukuda T, Hattori S, Arai F *et al*. Characteristics of optical actuator-servomechanisms using bimorph optical piezoelectric actuator[C]. In: *Proceedings of IEEE International Conference on Robotics and Automation*. Atlanta, USA, 1993. 618-623.

[10] Fukuda T, Hattori S, Arai F *et al*. Performance improvement of optical actuator by double side irradiation [J]. *IEEE Transactions on Industrial Electronics*, 1995, 42(5): 455-461.

[11] Morikawa Y, Nakada T. Position control of PLZT bimorph-type optical actuator by on-off control[C]. In: *Proceedings of the 23rd International Conference on Industrial Electronics*, *Control and Instrumentation*. New Orleans, USA, 1997. 1403-1408.

[12] Poosanaas P, Tonooka K, Uchino K. Photostrictive actuators[J]. *Mechatronics*, 2000, 10(4/5): 467-487.

[13] Liang L, Wang S, Cao F. Research on dynamic characteristic of optical drive servo system with PLZT[C]. In: *Proceedings of the Sixth International Symposium on Instrumentation and Control Technology*. Beijing, China, 2006. 63573T1-63573T6.

[14] Sun D, Tong L. Theoretical investigation on wireless vibration control of thin beams using photostrictive actuators[J]. *Journal of Sound and Vibration*, 2008, 312(1/2): 182-194.

[15] Tzou H S, Chou C S. Nonlinear opto-electromechanics and photodeformation of optical actuators[J]. *Smart Materials and Structures*, 1996, 5(2): 230-235.

[16] Shih H R, Tzou H S, Saypuri M. Structural vibration control using spatially configured opto-electromechanical actuators[J]. *Journal of Sound and Vibration*, 2005, 284(1/2): 361-378.

[17] Wang X J, Yue H H, Tzou H S *et al*. Actuation characteristics and control of thin cylindrical shells laminated with photostrictive actuators[J]. *Journal of Vibration and Shock*, 2009, 28(9): 9-14 (in Chinese).

[18] Shih H R, Tzou H S. Photostrictive actuators for photonic control of shallow spherical shells[J]. *Journal of Smart Materials and Structures*, 2007, 16: 1712-1717.

[19] Shih H R, Tzou H S. Wireless control of parabolic shells using photostrictive actuators[C]. In: *Proceedings of IMECE'2006*. Chicago, USA, 2006. 1507-1516.

[20] Tzou H S. *Piezoelectric Shells*[M]. Kluwer Academic Publishers, Boston, USA, 1993.

[21] Zhang Yimin. *Mechanical Vibration*[M]. Tsinghua University Press, Beijing, China, 2007 (in Chinese).